The negative impact of anode resistance on SiPMs as VLC receivers

William Matthews
Engineering Science
University of Oxford
Oxford, United Kingdom

Steve Collins
Engineering Science
University of Oxford
Oxford, United Kingdom

***Abstract*— The process used to detect individual photons in passively quenched Silicon Photomultipliers (SiPMs) creates a nonlinear response. A model is presented to show this nonlinearity is an unavoidable consequence of microcells recharging after a detection. However, results are presented which show the nonlinearity is increased by the inclusion of an anode readout resistor. Removal of this resistor improves ambient light performance of communication links by a factor of 1.9 under 300 mWm^{-2} of total 405 nm irradiance.**

Keywords—Silicon Photomultiplier, SiPM, Optical Wireless Communications, Visible Light Communications

I. Introduction

Silicon Photomultipliers (SiPM) are solid-state devices, capable of detecting individual photons. The structure of the SiPM is made by tiling multiple single photon avalanche diodes (SPADs), with quenching circuitry to create unit cells, on a common silicon substrate. Each unit cell, also known as a microcell, has the ability to independently detect single photons.

The SiPM has found many industrial applications including distance measurements in LIDAR, time of flight positron emission tomography, lifetime fluorescence spectroscopy, as well as applications in detectors for astrophysics and high energy physics [1].

A recent new application for SiPMs has been as extremely sensitive receivers for visible light communication (VLC) [2-8]. VLC is actively investigated as a technology which could augment or replace or replace existing radio frequency (RF) wireless infrastructure.

Deploying robust links within eye-safe limits is key for VLC. At the receiver, the bit error rate (BER) performance of an optical link depends on the signal to noise ratio (SNR) and the bandwidth of the detector. SiPMs can increase the link SNR with a limited transmitter irradiance, through a high gain which allows for photon counting. This capability allows for achieving sufficiently low BERs at transmitter irradiances close to the Poisson limit with on-off keying (OOK) [3]. SiPMs also achieve this sensitivity at a sufficiently high bandwidth to support gigabit per second communications. Prior work has shown that at 1 Gbps and a BER of 10^{-3}, a SiPM receiver has a 9 dB higher optical sensitivity than the best receiver based upon an avalanche photodiode [3].

In recent work, SiPMs have also demonstrated data rates up to 3.4 Gbps with OOK [4], however all the research presented has been performed on evaluation boards with a series readout resistor, which causes detrimental effects to the performance of the SiPM. A new device is presented without this resistor and is compared to measure any performance improvements.

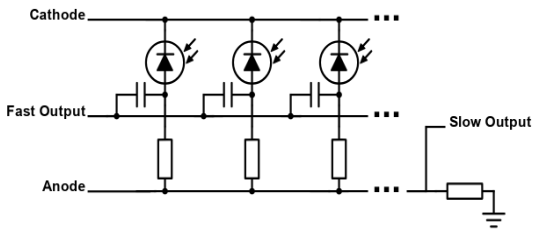

Fig.1. Schematic of On Semiconductor SiPM electrical layout

Despite being extremely sensitive to individual photons, the SiPM is inherently nonlinear in its response due to each microcell having to recharge after the detection of a photon. The associated time with this recharge process eventually causes the device to saturate and causes the photon detection efficiency and gain to change with optical power. This nonlinear response needs to be considered when devising pre- and post-equalization methods with OOK, and more importantly for the popular modulation scheme orthogonal frequency division multiplexing (OFDM).

OFDM is widely held as a preferred modulation scheme for VLC due to its high spectral efficiency, however it assumes a linear communications channel [5,9]. Any nonlinear characteristics cause harmonics, which is particularly a problem for OFDM which assumes each channel is linear and independent [5].

This paper is organized as follows. A description of SiPMs and their characteristics are discussed in Section II, and comparison between two SiPM evaluation boards are described in section III. Photon detection efficiency (PDE) is measured as a function of bias voltage, and hence a microcell is simulated in section IV. Data transmission experiments are presented in sections V and VI. Finally, section VII contains concluding remarks.

II. Description of SiPMs and their Characteristics

Under normal operation the SiPM is biased above the breakdown voltage V_{br}, which is when microcells begin to undergo avalanche multiplication. The bias voltage applied to the SiPM above the breakdown voltage is referred to as an overvoltage ($V_{over} = V_{bias} - V_{br}$).

When a photon is detected by a microcell, the SPAD undergoes avalanche multiplication, which creates an output pulse which can be counted. If the bias voltage over the SPAD is kept constant, the avalanche will continue and will be unable to detect another photon.

To reset the SPAD for detection of another photon, the avalanche must be arrested, which is typically performed by reducing the bias voltage over the SPAD. This is possible through either active quenching, which requires additional circuitry, or passive quenching, which is typically achieved by placing a resistor in series with the SPAD. In this work, only passively quenched SiPMs are considered, as the lack of

This manuscript was submitted to PRIME on February 18th, 2021. This work has been supported by the UK Engineering and Physical Sciences Research Council (EPSRC) under Grant EP/R00689X/1. W. Matthews (william.matthews@eng.ox.ac.uk) and S. Collins (steve.collins@eng.ox.ac.uk) are with the Engineering Science Department, University of Oxford, Oxford, UK.

978-1-6654-6700-1/22/$31.00

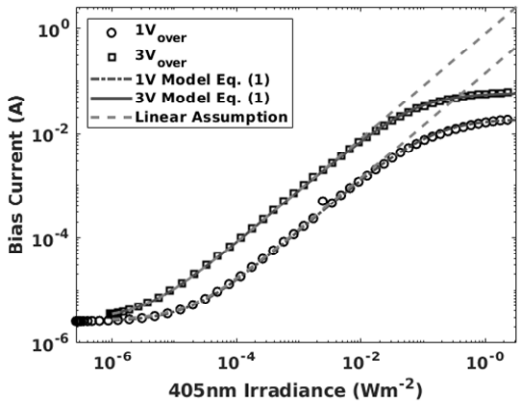

Fig. 2. The measured current needed to maintain an over-voltage of 1 V and 3 V on a 30020 MicroFJ series SMTPA package SiPM at different irradiances from 405 nm UV3TZ-405-15 LEDs.

additional circuitry associated with active quenching increases the active area of the device, and hence the photon detection probability.

Once current flows through the SPAD and hence the series microcell resistor, the bias voltage for that single SPAD is decreased below the breakdown voltage, halting the avalanche, and allowing the device to recharge.

Typically, the output of a SiPM is measured through circuitry in series with the anode of the device. This output, referred to as the slow output, allows measurement of the recharging current into the SiPM.

The SiPM used for this study was an On Semiconductor MicroFJ-30020. A unique feature of On Semiconductor's SiPMs is that they have a 'fast output'. This fast output is capacitively coupled to each microcell, giving a common analog output. The structure of On Semiconductor's SiPMs are detailed in Fig. 1. The fast output has a much narrower pulse width, which is due to capacitor coupled to each microcell passing the rapid avalanche process that occurs within the microcell on detection of a photon. In the context of VLC, for an acceptable bit error rate to be achieved, several photons need to be detected for each bit.

A model has been described in prior work [4], to model for output pulse rate $\dot{D}$:

$$\dot{D} = \frac{N_{cells}\,\alpha \cdot (L + L_{dark})}{1 + \alpha\tau \cdot (L + L_{dark})} \tag{1}$$

Where N_{cells} is the number of microcells, L and L_{dark} are the incoming irradiance and irradiance required to create the device's characteristic dark counts. The characteristic time τ is defined as 2.2 times the recharge time of the microcell. Finally, α is defined as

TABLE I
KEY PARAMETERS OBTAINED FROM THE MANUFACTURES DATA SHEET FOR A J SERIES 30020 WITH AN OVERVOLTAGE OF 5V [10]

Parameter	30020
Number of Microcells	14410
Microcell Active Area Diameter (μm)	20
Fill factor (%)	62
Microcell Recharge Time Constant (ns)	15 ns
PDE (405 nm)	0.38 (@ 5 V_{over})
Dark Count Rate (MHz)	1.2 (@ 5 V_{over})
Pulse Width (ns)	1.4

$$\alpha = \frac{\eta(V_{over}, \lambda) A_{\mathrm{SiPM}}}{E_p(\lambda) N_{\mathrm{cells}}} \tag{2}$$

Where $\eta(V_{over}, \lambda)$ is the PDE of the SiPM at a particular overvoltage V_{over} and wavelength λ. A_{SiPM} is the area of the device and E_p is the photon energy for a given wavelength. C_{cell} can be measured by assuming each microcell passes the same charge on detection of a photon $I_{bias} = Q_{cell}\dot{D}$, and using the assumption that each SPAD behaves as a capacitor $Q_{cell} = C_{cell}V_{over}$, Q_{cell} . By operating in the saturated region $\alpha\tau \cdot (L + L_{dark}) >> 1$, equation 1 simplifies to a maximum count rate,

$$\dot{D}_{max} = \frac{N_{cells}}{\tau} \tag{3}$$

which can be combined with the above assumptions for a measurement of cell capacitance.

$$C_{cell} = \frac{I_{bias}\tau}{N_{cells}V_{over}} \tag{4}$$

A microcell capacitance of 43 fF was determined by measuring the saturation current at 34 overvoltages from 0.5 V to 3.9 V and fitting a line with least squares.

Keeping bias voltage constant, a bias current-irradiance curve can hence be shown in Fig. 2. The model in equation 1 was fitted for both tested overvoltages, using data from Table I, measurement of the recharge time for the SMA board [4] and a fitted L_{dark} of 3.4 μWm^{-2}.

To measure the PDE $\eta(V_{\mathrm{over}}, \lambda)$ from a measurement of the bias current, the device must be in the linear region $\alpha\tau \cdot (L + L_{dark}) << 1$ with $L >> L_{dark}$. The following simplification of the model in equation 1 can hence be used

$$\eta(V_{\mathrm{over}}, \lambda) \approx \frac{E_p(\lambda)\, I_{bias}(V_{\mathrm{over}}, L)}{C_{cell}V_{\mathrm{over}}A_{\mathrm{SiPM}} \cdot (L + L_{dark})} \tag{5}$$

III. Comparison of SMTPA and SMA Evaluatoin Boards

On Semiconductor offers SiPMs on a surface mount technology pin adaptor (SMTPA) evaluation board, which consists of the SiPM mounted on a small circuit board with RF header pins to plug directly into another circuit board.

On Semiconductor also offers the MicroFJ series of SiPM on a SMA evaluation board, which permits access to both the fast and slow outputs as seen on Fig. 1. This SMA evaluation board exists to aid users in assessing the technology in a convenient manner and has consequently been used for prior

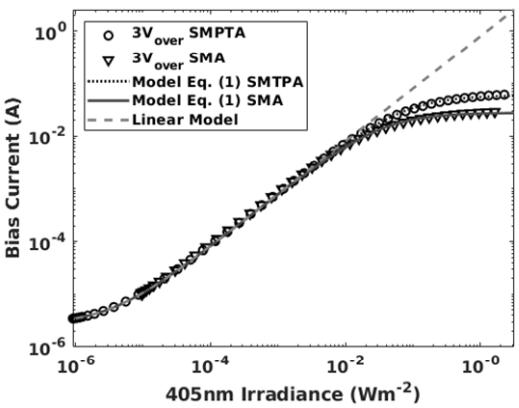

Fig. 3. The measured current needed to maintain an over-voltage of 3V on a 30020 MicroFJ series SMTPA and SMA SiPM at different irradiances from 405 nm LEDs.

work in VLC [2-5,8]. The SMA evaluation board has a 50 Ω resistor in series with the anode of the SiPM, to for allow measurement via the slow output of the current flowing through the SiPM to recharge the microcells. Under high irradiances, causing saturation, the current flowing through this 50 Ω resistor causes the SiPM overvoltage to drop as much as 1.5 V.

The SMA evaluation board's recharge time was measured to have a full width half max time of 30 ns, however the data sheet of the device presents a recharge time of 15 ns when a 1 Ω resistor is instead present in series with the anode [4].

The SMTPA evaluation board allows direct access to the anode of the SiPM, which when grounded prevents the significant overvoltage drop as seen on the SMA board. When the anode is connected directly to ground, it is not possible to measure the recharge current of a microcell, and hence measure the recharge time. The datasheet value of 15 ns was therefore used for the model (1).

When the evaluation boards are compared directly on a bias current-irradiance plot in Fig. 3, both boards perform equally in their linear region until approximately 30 mWm^{-2}. In saturation, the SMA board has a lower bias current, caused by the longer recharge time. At 1 Wm^{-2} the SMTPA board has a bias current of 56.7 mA, a factor of 2 times the SMA board's bias current of 28 mA. Comparing to the recharge times of the devices, the SMTPA board has a recharge time half of the SMA board's measured recharge time. As both fits have the same PDE of 0.34, the reduced PDE from the overvoltage decreasing does not have a significant impact.

IV. Microcell Simulation

The PDE as a function of overvoltage when the irradiance from the 405nm LED ring was 2.4 mWm^{-2} was also measured. The overvoltage was varied between 0.5 V to 3.9 V in 100 mV increments, and the bias current measured.

The measured relationship between the PDE and the device overvoltage was obtained by using equation (5). An empirical model was hence fitted for the PDE as a function of the overvoltage V_{over},

$$\eta(V_{over}, 405nm) = 0.46\left(1 - exp\left(\frac{-V_{over}}{0.083V_{br}}\right)\right) \quad (6)$$

Where V_{br} is the breakdown voltage, and the coefficient of 0.46 is specific to a wavelength of 405 nm. When compared, both SMA and SMTPA evaluation boards showed identical PDE-overvoltage characteristics. When measured for a particular irradiance in the linear region, as the overvoltage increases, the PDE rises.

A time-domain simulation was made to fully model the SiPM's recharging process, and hence its PDE dependence on overvoltage. The simulation consists of an array of times since the last detected photon. From this time array, a microcell overvoltage and hence charge can be calculated assuming RC time constant recharging.

$$V_{microcell}(t) = V_{over}\left(1 - exp\left(\frac{t}{\tau}\right)\right) \quad (7)$$

For each simulation time step, the microcell PDE is hence calculated from this overvoltage using the model in equation (6). Microcells are uniformly, randomly struck by photons which randomly experience detections depending on the microcell's PDE. On detection of a photon, the microcell's time since last detected photon is set to zero. This behavior

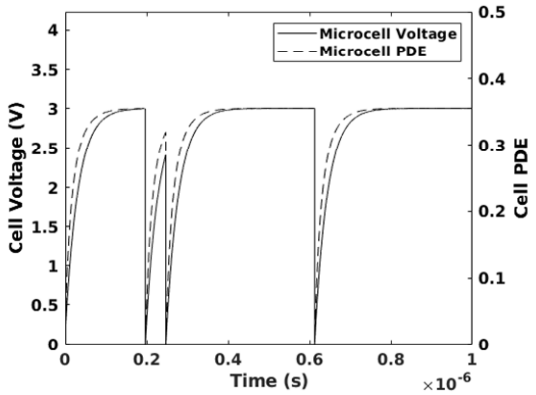

Fig. 5. Time domain simulation of a single Micro FJ 30020 SMTPA microcell under 5mWm^{-2} of 405nm irradiance.

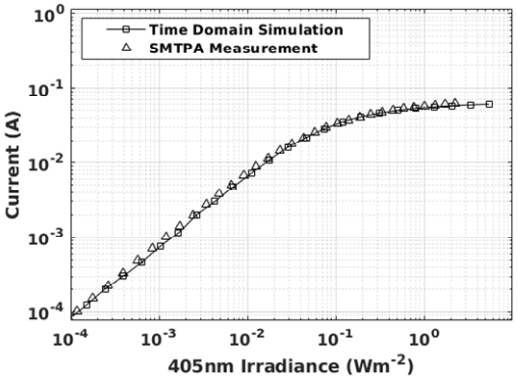

Fig. 6. Simulated current needed to maintain an overvoltage of 3V on a Micro FJ 30020 SMTPA SiPM.

results in a time domain simulation shown in Fig 5, which gives a view of a microcell under 5 mWm^{-2} of constant light. Despite a photon being detected when the device has not fully recharged, an output pulse is still generated. A bias current-irradiance curve can hence be simulated from the model, by summing the charge in microcells which detect a photon. Fig.6 shows the simulated bias current-irradiance curve for a MicroFJ-30020 SMTPA SiPM. The simulation agrees with the measured results, which suggests the PDE model and recharge profile are valid approximations.

V. Data Transmission Experiment Set Up

A Tektronix 70002A Arbitrary Waveform Generator (AWG) was used to generate a pseudorandom binary sequence (PRBS) OOK signal. This signal was then amplified by a Fairview FMAM3269 amplifier to produce a 2 V_{pp} signal. 8b10b coding was used as this amplifier has a bandpass beginning at 10 MHz. This signal was combined with a DC bias of 35.5 mA in a Mini Circuits Bias-Tee ZFBT-4R2GW+, which was applied to a L405P20 laser diode, which has an output center wavelength of 405 nm. A wavelength of 405 nm was chosen as it is the wavelength with the highest PDE for the J-Series SiPMs.

The light from the laser diode passes through a collimating lens, polarizer and into a multi-mode fiber to the transmitter assembly. The transmitter assembly consists of a collimating lens and a ground glass diffuser to create a uniformly illuminated area where the receiver is placed.

A ring of eight UV3TZ-15 LEDs was used as a background 405 nm irradiance source, which was controlled by a Keithley

224 source measure unit. The irradiance at the receiver was measured with an 818-UV calibrated photodiode.

The receiver consisted of a SiPM cooled with a fan, which was biased by a programmable bench power supply. The fast output was connected to a ZX60-43-S+ 4GHz amplifier, which was then connected to a Keysight MSO64 4 GHz oscilloscope. The captured waveform was then post-processed in MATLAB®, by low pass filtering, and applying decision feedback equalization (DFE) to compensate for ISI. Finally, the BER was calculated and used as feedback to adjust the transmitter irradiance through moving the polarizer to achieve a target BER.

VI. Data Transmission Results

Data transmission experiments over a distance of 40 cm were performed at a data rate of 500 Mbps. Due to the finite width of the SiPM output pulses and other transient effects, the system suffers from inter-symbol interference and therefore DFE was employed before the BER was calculated.

Ambient 405 nm light illuminating the SiPM from the LED ring was varied between 2 mWm^{-2} and 1 Wm^{-2}. The irradiance from the transmitter was then varied using a polarizer until a BER of $3.8{\cdot}10^{-3}$ (a 7% forward error correction limit) was achieved at each background irradiance.

Fig. 7 shows the SMTPA and SMA evaluation boards' performance under ambient illumination. The SMTPA board required a lower transmitter power than the SMA board for all tested irradiances. To sustain a BER of $3.8{\cdot}10^{-3}$ at 500 Mbps, for a total irradiance between than 2 mWm^{-2} and 300 mWm^{-2}, the relationship between the required transmitter irradiance L_{TX} and total irradiance incident L_{Total} on the SMA evaluation board SiPM is $L_{\mathrm{TX}} = 0.14 \times L_{\mathrm{Total}}^{0.7}$.
For the SMTPA board, the relationship is $L_{\mathrm{TX}} = 0.06 \times L_{\mathrm{Total}}^{0.58}$.

The SMTPA board required a lower transmitter power for the entire tested range. The transmitter power also scaled more slowly with an increase in incident ambient light. When the total irradiance illuminating the SiPM is above 300 mWm^{-2}, the SMA evaluation board required a factor of 1.9 times more transmitter power than the SMTPA board.

VII. Conclusion

This paper investigated the penalty associated with anode resistance on the Fast Output of On Semiconductor SiPMs.

A bare J-Series SiPM experiences approximately 1 Wm^{-2} of 405 nm equivalent irradiance when exposed to 500 lux of WLED light [8]. Adding a filter pack (BG3, a BG39 and a B370) leads to an ambient light suppression by three orders magnitude (0.8mW m^{-2} of 405 nm equivalent irradiance) [8]. The reduction of ambient light level allowed for an in-depth analysis of the anode resistance of SiPMs. It has been shown that the recharge time decreases with decreasing anode resistances. The reduction of recharge time allows for a higher overall bandwidth, and improved saturation performance. Moreover, the lower recharge time allows for a higher time-average PDE. The lower recharge time means the SMTPA board is closer to an ideal device for research purposes, more consistent measurements can be obtained, and the performance of VLC links is improved.

The SMTPA board SiPM also allows the possibility of combining multiple SiPMs together, to create a larger device

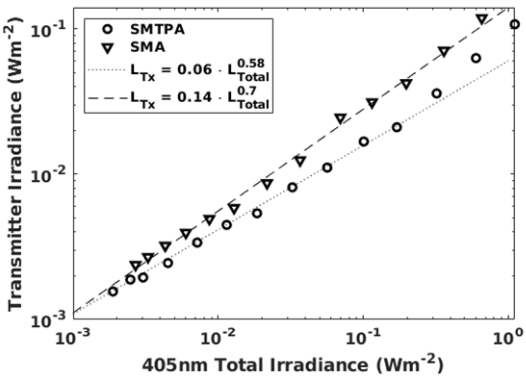

Fig. 7. Transmitter irradiance required to support a 500 Mbps link under varying 405 nm background light.

without the penalty of increased pulse width, and hence reduced bandwidth. If ideal photon counting conditions are achieved without a bandwidth limitation, the number of detected photons per bit determines the error rate. Hence the data rate scales with the number of SiPMs,

While a SiPM with a lower recharge time and thus higher maximum count rate is beneficial, the inherent nonlinearity from microcells recharging is still a concern for the main modulation schemes in VLC, OOK and OFDM. Understanding this nonlinearity will result in the development of optimal pre- and post-equalization methods, which is essential in paving the way for high-speed VLC transmission when operating in challenging environments.

References

[1] Gundacker, Stefan, and Arjan Heering. "The silicon photomultiplier: fundamentals and applications of a modern solid-state photon detector." in *Physics in medicine and biology* vol. 65,17 17TR01. 21 Aug. 2020, doi:10.1088/1361-6560/ab7b2d

[2] W. Ali, G. Faulkner, Z. Ahmed, W. Matthews, D. O'Brien and S. Collins, "Silicon photomultiplier receivers and future VLC systems," *2020 IEEE Globecom Workshops* (GC Wkshps, 2020, pp. 1-5, doi: 10.1109/GCWkshps50303.2020.9367590.

[3] Z. Ahmed, R. Singh, W. Ali, G. Faulkner, D. O'Brien and S. Collins, "A SiPM-Based VLC Receiver for Gigabit Communication Using OOK Modulation," in *IEEE Photonics Technology Letters*, vol. 32, no. 6, pp. 317-320, 15 March15, 2020

[4] W. Matthews, et al. "A 3.45 Gigabits/s SiPM-Based OOK VLC Receiver." in *IEEE Photonics Technology Letters*, vol. 33, no. 10, Institute of Electrical and Electronics Engineers, 2021, pp. 487–90.

[5] W. Matthews, C. He and S. Collins, "DCO-OFDM Channel Sounding with a SiPM Receiver," *2021 IEEE Photonics Conference (IPC)*, 2021, pp. 1-2, doi: 10.1109/IPC48725.2021.9592851.

[6] H. Zimmermann, "APD and SPAD Receivers: Invited Paper," *2019 15th International Conference on Telecommunications (ConTEL)*, Graz, Austria, 2019, pp. 1-5, doi: 10.1109/ConTEL.2019.8848547.

[7] L. Zhang, D. Chitnis, H. Chun, S. Rajbhandari, G Faulkner, D. O'Brien and S. Collins.., "A Comparison of APD- and SPAD-Based Receivers for Visible Light Communications," in *Journal of Lightwave Technology*, vol. 36, no. 12, pp. 2435-2442, 15 June15, 2018, doi: 10.1109/JLT.2018.2811180.

[8] Ali, W., et al. "Giga-Bit Transmission between an Eye-Safe Transmitter and Wide Field-of-View SiPM Receiver." in *IEEE Access*, vol. 9, IEEE, 2021, pp. 154225–36.

[9] Viola, S., Islim, M. S., Watson, S., Videv, S., Haas, H., & Kelly, A. E. (2017). "15 Gb/s OFDM-based VLC using direct modulation of 450 GaN laser diode," Proc. SPIE 10437, Advanced Free-Space Optical Communication Techniques and Applications III, 104370E (6 October 2017); https://doi.org/10.1117/12.2292004

[10] Onsemi.com. 2020. *J-Series SiPM Sensors Datasheet*. [online] Available at: https://www.onsemi.com/pub/Collateral/MICROJ-SERIES-D.PDF, Accessed 10 March 2020